DNA Charge Transfer: An Atomistic Model

Tobias Cramer, Sebastian Krapf, and Thorsten Koslowski*

Institut für Physikalische Chemie, Universität Freiburg, Albertstrasse 23a, D-79104 Freiburg im Breisgau, Germany

Received: January 20, 2004; In Final Form: April 16, 2004

In this work, we address the phenomenon of charge transport in DNA using a simple, but chemically specific, approach that is intimately related to the Su-Schrieffer-Heeger (SSH) model. The emerging potential energy surface for hole transport is analyzed using Marcus' theory of charge transfer. Our results are fully compatible with the conjecture of charge transfer in DNA via two competing mechanisms, and the computations provide the corresponding charge-transfer rates both in the short-range superexchange and in the long-range hopping regime as the output of a single atomistic theory. Finally, the model allows the computation of the transport properties of systems containing modified bases and of more complex arrangements of base pairs as an additional element of verification.

1. Introduction

The past decade has seen a considerable growth of interest in charge transport within deoxyribonuleic acid (DNA).[1,2] Understanding the direction of mutations upon oxidative stress or UV irradiation via the migration of charges to preferential sites of trapping, potential sensor applications, and the prospect of having a nanosized biopolymer wire at hand that can be easily replicated are tantalizing perspectives and have motivated many experimental and theoretical studies.

From an experimental point of view, three approaches have to be distinguished. In a series of landmark photochemical studies, Barton and co-workers have pioneered charge mobility studies in DNA by intercalating donor and acceptor complexes into DNA strands.[3] The analysis of the photochemical kinetics, now possible down to the femtosecond range,[4] has helped to gain a deeper understanding on the mechanism of charge transfer in the excited state. More recently, Giese and co-workers have oxidatively created holes in DNA and have studied their migration by analyzing the products resulting from the consecutive reactions.[5] In a third type of experiment, a DNA strand is connected to two electrodes. The application of a potential deforms the DNA valence and conduction bands until coherent transport sets in.[6] In this way, the band gap and the mobility of the charge carriers can be determined. Photochemical charge separation, the creation of excess charges (which is equivalent to a doping process in the terminology of solid-state physics), and transport measurements in nanodevices all address the same question, whether DNA can support rapid and long-range charge transfer, but in different time and energy regimes.

For the experiments of the Giese group, a phenomenological hopping model has been developed by Bixon et al.,[7] which rationalizes DNA hole transport in terms of interbase hopping and trapping. From this model, the following picture emerges: multistep hopping occurs only between guanine bases, which act as traps due to their low oxidation potential, and intervening A−T base pairs give rise to tunneling via a superexchange mechanism. Recently, Giese and co-workers have introduced elements of long-range transport into their kinetic model.[9] Renger and Marcus have presented an approach that involves tunneling, hopping, and an intermediate regime;[8] a related theory for bridge-mediated charge transfer has also been suggested by Petrov et al.[10] A variety of quantum chemical calculations on nucleobase oligomers (typically two or three base pairs in the B form) exists, which lead to numerical estimates of the energy parameters that enter Marcus' theory of charge transfer in two-site donor−acceptor systems.[11] These studies comprise computations of the electronic tunnel splitting,[12−14] the ionization potentials,[15] and the reaction enthalpy.[15,16] With the help of these approaches, considerable new theoretical insight into the mechanism of DNA charge transfer has been obtained. Nevertheless, a central question of charge transport in DNA remains unanswered: Does a unified, microscopic, nonphenomenological theory exist which accounts for both the superexchange and the long-range transport mechanism?

In the work presented here, we focus on the energetics of hole transfer in DNA in the electronic ground state and thus address aspects of transport intimately related to those studied experimentally by Giese's group. In particular, we aim at the computation of the aforementioned energy parameters resulting from a single, simple, flexible, and chemically specific model Hamiltonian that allows a full variational control. The remaining part of our work is organized as follows. In the next section, we motivate and introduce the model Hamiltonian and its parametrization using ab initio density functional calculations. In the third section, cross-sections of the emerging potential energy surface relevant to hole transfer are computed and analyzed. The results are discussed and compared to experiments. Conclusions are derived in the final section.

2. Model

As geometries, we use models of the A and B forms of DNA as generated by the NUCLEIC program of Ponder's TINKER suite.[17] In their default form, they correspond to the bulk structure of DNA fibers with a different water content. We consider these geometries as a sufficient basis to test whether our implementation of the SSH model, as described below, is a valid model for hole transfer in DNA. We are aware of the

* To whom correspondence should be addressed. E-mail: Thorsten.Koslowski@physchem.uni-freiburg.de. Fax: (+49)761-203-6189.

10.1021/jp049712s CCC: $27.50
Published on Web 07/09/2004

facts that both DNA forms may exhibit a distorted geometry at the end of the finite strands studied here and that disorder phenomena may play an important role in charge transfer.[1,14,18]

In this work, we assume that the nucleobases with their high-energy frontier molecular orbitals dominate the charge transport properties, and we hence neglect the deoxyribose and the phosphate units beyond their role of providing a scaffold for the base pairs. By removing these entities from the structure, dangling bonds are created, which have been saturated by hydrogen atoms. As the isolated bases are planar and the interbase tight-binding matrix elements are small, as will be demonstrated below, the $\sigma-\pi$ separation approximately holds, and theories of the chemical bond approriate to π systems can be applied. In the field of conductivity phenomena in π systems, the Su-Schrieffer-Heeger (SSH) model[19] has shown a remarkable track of success, in particular for conducting polymers such as polyacetylene. In addition, we note that applications to molecular systems,[20] carbon nanotubes,[21,22] and complex systems[23] exist. In its standard form, the SSH Hamiltonian reads

$$\hat{H} = \sum_i \frac{m\dot{x}_i^2}{2} + \sum_{\langle ij \rangle} \frac{k}{2}(x_i - x_j)^2 - \sum_{\langle ij \rangle} [t_0 - \alpha(x_i - x_j)](a_i^\dagger a_j + a_j^\dagger a_i) \quad (2.1)$$

where $x_i - x_j$ denotes the deviation of the distance between a neighboring pair of atoms from that of a carbon−carbon single bond, k is the corresponding force constant, t_0 is the tight-binding coupling matrix element, and α denotes the electron−phonon coupling constant. The angular brackets indicate the restriction of the sum to distinct pairs of neighbors, and the $a_i^\dagger/a_i$ are creation/annihilation operators acting on a basis of atomic orbitals, which is assumed to be orthogonal. As standard in the SSH model, nuclear coordinates and momenta are treated as classical quantities.

The SSH Hamiltonian can be separated into an electronic and a nuclear part using a displaced phonon coordinate.[22] Within the restricted Hartree−Fock mean field approximation, the transformed electronic part of the Hamiltonian is given by[22]

$$\hat{H} = -\sum_{\langle ij \rangle} (t_0 + 4U_{\mathrm{SSH}}\bar{n}_{ij})(a_i^\dagger a_j + a_j^\dagger a_i) + 4U_{\mathrm{SSH}} \sum_{\langle ij \rangle} \bar{n}_{ij}^2 \quad (2.2)$$

where the $\bar{n}_{ij}$ are the tight-binding bond orders (which are proportional to the displacements $x_i - x_j$ of the original SSH model), and we define the so-called off-diagonal Hubbard parameter $U_{\mathrm{SSH}} = \alpha^2/2k$, which is equal to 0.32 eV in the standard SSH model. The Hamiltonian 2.2 accounts for the chemical bond within the bases and inner sphere contributions to the charge-transfer reaction via a possible change in the bond orders or bond lengths.

To describe the influence of solvent polarization effects, we apply a straightforward extension of Marcus' treatment of the energetics of outer-sphere reactions[11] to many-site systems. We write the reorganization energy emerging from an ensemble of excess charges Δz_i localized within spheres of radii σ_i as

$$\lambda_{\mathrm{out}} = \frac{e^2}{4\pi\epsilon_0}\left(\frac{1}{\epsilon_\infty} - \frac{1}{\epsilon_s}\right)\left(\sum_i \frac{\Delta z_i^2}{\sigma_i} - \sum_{i<j} \frac{\Delta z_i \Delta z_j}{r_{ij}}\right) \quad (2.3)$$

If the high- and the low-frequency dielectric response characterized by the constants ϵ_∞ and ϵ_s can be separated and the long-range Coulomb interactions are neglected, this model turns into the interaction term of a spin-free Hubbard Hamiltonian.[24] We replace the charges Δz_i by the corresponding number operators and arrive at

$$\hat{H}_{\mathrm{ee}} = -U_{\mathrm{ee}} \sum_i (n_i - n_{i,0})^2 \simeq -U_{\mathrm{ee}} \sum_i [2n_i(\bar{n}_i - \bar{n}_{i,0}) - \bar{n}_i^2 + \bar{n}_{i,0}^2] \quad (2.4)$$

where the right hand side again results from a mean-field approximation to the interaction. It can be interpreted as a nonretarded reaction field, which extends the linear combination of atomic orbitals (LCAO) approach to systems embedded in a polarizable environment.[25,26] In this work, we use $U_{\mathrm{ee}} = 0.8$ eV, a choice that will be motivated in the following section. U_{ee} is the only adjustable parameter of our model. As it incorporates the internal reaction field parameters σ, ϵ_s, and ϵ_∞, these quantities do not have to be parametrized explicitely. As an upper limit of U_{ee}, we consider the value of 1.2 eV obtained by Utz and Koslowski[25] and applied by Koslowski et al.[28] to charge localization and hopping in a π orbital system in the absence of off-diagonal electron−phonon coupling. In that case, U_{ee} has to absorb the attractive off-diagonal effects and is thus larger than the pure diagonal U_{ee} in the presence of SSH electron−phonon coupling terms. The combined Hamiltonians 2.2 and 2.4 can be solved self-consistently. In this case, the $\bar{n}_{ij}$ and $\bar{n}_i$ are computed from a previous self-consistent field (SCF) step.

The introduction of a displaced phonon coordinate and the replacement of charges by the corresponding number operators hold in the nonretarded or zero-frequency limit.[30] In this context, we have to note that we are aware of the complex dynamical problems inherent to charge transfer and the difficulties of integrating out a large number of bath or internal degrees of freedom on different time scales.[31] Adiabatic charging schemes[32,33] related to our approach have, however, greatly advanced the theoretical treatment of complex systems that exhibit electron transfer, and the immediate, or nonretarded, response from the vibrational and polarization degrees of freedom that enter the expressions 2.1 and 2.3 is tantamount to an adiabatic interpretation of charge transfer, on which we will focus here. As will be illustrated below, the approach presented here renders the computation of effective parameters describing charge hopping and transfer possible even for complex many-orbital systems. These effective parameters, obtained not from a phenomenological but an atomistic description of the system, can then be used to compute experimentally observable properties within the framework of theories available for two-site electron transfer. This approach has been applied to charge-transfer problems in a variety of systems.[25−28]

The application of a retarded reaction field implies a delayed response of polarization or vibrational degrees of freedom to the hopping charge. If this response is sufficiently slow, the inverse hopping frequency will eventually become smaller than the time scale relevant to the trapping process, and the excess charge is dynamically delocalized, as for example quantified by one of us in a simple analytical approach to this problem.[27] As a consequence, the reaction field strengths U_{ee} and U_{SSH} are dynamically screened. This screening effect is a function of the temperature, and at a critical T_C, the charge may become detrapped provided the effective tunnel splitting t is sufficiently strong. The crossover region between the localized regime, where the screened U parameters are close to their zero-temperature limits, and the delocalized regime, where $U < t$ holds, is, however, small.[27] Thus, within the localized regime,

the screened U parameters can be considered as constant. This argument is also substantiated by conductivity measurements on solids that exhibit a Verwey transition from a localized to a delocalized mixed valence character. Here, the conductivity below T_C shows Arrhenius behavior (see, e.g., ref 29) with a temperature-independent activation barrier and hence a constant $U \simeq 2E_A$. To our knowledge, all experiments on DNA conductivity suggest a mechanism typical for the localized regime (i.e., superexchange or adenine-adenine intermediate hopping). Hence, we are confident that U_{ee} and U_{SSH} can be treated as constants and that the nonretarded approximation holds.

As the standard SSH model only describes hydrocarbons, a chemically specific modification is required to handle the heterocyclic nucleobases, which also contain nitrogen and oxygen atoms. We introduce the valence orbital ionization potentials for oxygen and two types of nitrogens, distinguished by their coordination numbers as N2 and N3, as additional diagonal parameters ϵ_i of the Hamiltonian 2.2 via $\hat{H}_{diag} = \sum_i \epsilon_i a_i^\dagger a_i$. In π electron theories, the C−N-bond matrix element is considered to be smaller than its C−C counterpart, and we set $t_{CN} = 0.8t_{CC}$.[34] The numerical values of the parameters have been obtained by a careful fit of the modified SSH model to ab initio density functional calculations of the nucleobases A, C, G, and U (here, we regard U as equivalent to T concerning the atoms that participate in π bonding). These reference calculations have been performed with the Gaussian 03 program package[35] using the B3LYP exchange-correlation functional and the 6-31G** split-valence basis set. The valence orbital 2p ionization potentials with reference to carbon (ϵ_O, ϵ_{N2}, ϵ_{N3}) and the t_{CC} tight-binding matrix element are interpreted as global parameters independent of the base, whereas shifts of the entire spectrum for the individual bases (ΔE_A, ΔE_C, ΔE_G, ΔE_U) are permitted. Within the calibration procedure, the root-mean-square deviation between the occupied ab initio and SSH π orbital energy levels

$$\sigma = \frac{1}{n_{occ}} \sqrt{\sum_{\mu=1}^{n_{occ}} (\lambda_\mu^{DFT} - \lambda_\mu^{SSH})^2} \qquad (2.5)$$

has been minimized. We have not considered the one-electron excited states for the parametrization procedure, because the DFT vacant orbitals are generally less accurate than their occupied counterparts, and as we intend to study hole transfer, which emerges from the creation of a hole in the highest occupied molecular orbital (HOMO), which is separated from the lowest vacant state by a considerable energy gap. For the parameters that are independent of the bases, we have obtained $t_{CC} = -2.873$ eV, $\epsilon_O = -2.254$ eV, $\epsilon_{N2} = -1.502$ eV, and $\epsilon_{N3} = -4.504$ eV. The root-mean-square (RMS) deviations amount to $\sigma_A = 7 \times 10^{-2}$ eV, $\sigma_C = 8 \times 10^{-2}$ eV, $\sigma_G = 6 \times 10^{-2}$ eV, and $\sigma_U = 9 \times 10^{-3}$ eV, respectively. Considering the simplicity of the underlying model and the small number of parameters required, these RMS values are more than satisfying; with an order of magnitude approaching 0.1 eV ≃ 10 kJ/mol, they do, however, not give rise to thermodynamic accuracy, which cannot even be expected from the reference computations. We obtain a sequence of $E_G^0 < E_A^0 \simeq E_C^0 < E_U^0$ for the adiabatic SSH oxidation potentials. The computed oxidation potentials mainly depend on the HOMO energies. A small shift of the entire set of adenine (+0.25 eV) and cytosine (−0.16 eV) SSH energy levels leads to a quantitative agreement of the computed and the experimental relative oxidation potentials,[36] $\Delta E_{AG}^0 = E_A^0 - E_G^0 = 0.47$ eV, $\Delta E_{GA}^0 = 0.18$ eV, and $\Delta E_{UC}^0 > 0.25$ eV. The base-specific energy shifts finally amount to $\Delta E_A = -3.73$ eV, $\Delta E_C = -3.95$ eV, $\Delta E_G = -4.00$ eV, and $\Delta E_U = -4.52$ eV. The results presented in the following section do not require precise values for the ΔE_i, provided that G exhibits the lowest oxidation potential, which is the case both in the absence and the presence of additional energy shifts for A and C. Figure 1 may serve as a graphical summary of the parametrization, and it depicts the SSH energy levels as a function of the DFT orbital energies.

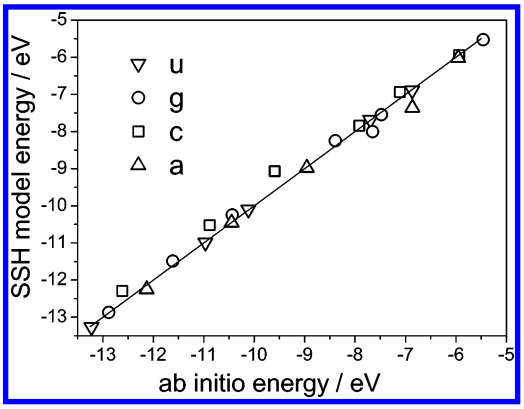

Figure 1. Energies of the occupied π molecular orbitals of the bases A, C, G, and U. SSH energy levels as a function of the reference energies computed within an ab initio study.

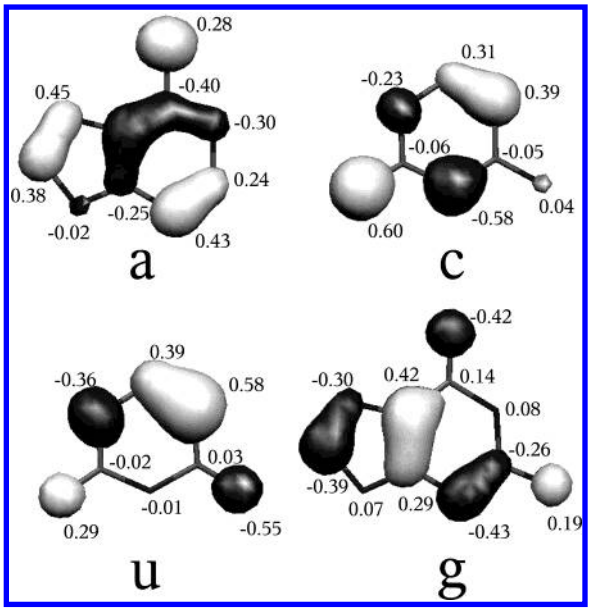

Figure 2. Highest occupied molecular orbitals of the bases A, C, G, and U. The isosurfaces have been computed from the ab initio eigenfunctions, and the numbers are the molecular orbital coefficients of the SSH model calculations.

Finally, an assessment of the quality of the parametrization beyond the orbital energy RMS values, eq 2.5, is possible. As the hole is created in the HOMO of the SSH model, this molecular orbital should exhibit a close similarity to its ab initio counterpart. In Figure 2, we display graphical representations of the ab initio A, C, G, and U HOMOs utilizing the MOLEKEL program[37] and the corresponding SSH atomic orbital (AO) coefficients as numerical values. We note that for all bases, not only the sign of the AO contributions to the HOMO and its nodal structure are well represented but that with the exception of the central (here: negative) part of adenine the numerical values of the SSH HOMOs also provide a very good description of the highest occupied DFT orbital.

We now turn to the parametrization of the long-range interactions between the bases, which is again performed using

results from ab initio computations. As a simple model solely used for the parametrization of the interactions, we take two identical bases which are oriented in parallel and carry a positive charge.[12] The occupied π orbitals of these molecules overlap, and the orbitals, which are degenerate in the absence of such interactions, split energetically. This splitting has been obtained by Voitjuk et al. within a Hartree−Fock computation (using 6-311G** as the most advanced basis set) at separations of 2.88, 3.28, and 3.88 Å.[12] Due to its orientational character, the interaction is dominated by a σ overlap, which we assume to be of an exponential dependence upon the interatomic distances, $V_{pp\sigma} = V^0_{pp\sigma} \exp(-\alpha r)$. We postulate the same type dependence upon distance for long-range π interactions, which mainly become operative between the two nucleobases that form a Watson−Crick pair, and use $V^0_{pp\sigma}/V^0_{pp\pi} = -0.268$.[38] The parameters of the model interaction have been optimized to meet the ab initio results, and we finally arrive at $\alpha = 1.45$ Å^{-1} and $V^0_{pp\sigma} = 43.2$ eV. We note that for the coupling matrix elements between bases of oligomers that mimic the DNA B form, the results of Voityuk et al.[12] and those of Troisi and Orlandi[13] exhibit only small differences.

To account for the nonparallel orientation of the bases, the AOs participating in π bonding are taken as hybride orbitals, $|p_{ia}\rangle = \sum_{k=1}^{3} c_{kia}|p_{kia}\rangle$ with $k = x$, y, or z. The vector $\vec{c}_{ia}$ is constructed orthogonal to the base a under consideration, and the interaction between two hybride orbitals located on different bases a and b can be computed via

$$\langle p_{ia}|\hat{H}|p_{jb}\rangle = \sum_{k=1}^{3}\sum_{l=1}^{3} c_{kia}c_{ljb}\langle p_{kia}|\hat{H}|p_{ljb}\rangle \qquad (2.6)$$

where the orientational dependence of the right-hand side of this equation can be evaluated using the familiar Slater-Koster rules.[39] In this manner, configurations of nucleobases in an arbitrary orientation can be studied, and a reparametrization is not required if new model geometries are introduced.

We note that the application of the SSH model to charge-transfer problems in DNA has been pioneered by Conwell and Rakhmanova.[40] These authors have used the original SSH Hamiltonian and have represented each base pair by a single site. Between these sites, tight-binding and electron−phonon interactions occur. With parameters appropriate to DNA, polaron formation and polaron mobility in an electric field have been studied. The model presented here differs from the Conwell-Rakhmanova approach in the following aspects: we use an atomic representation of the nucleobases, and electron−phonon coupling is only assumed for covalent bonds. A reaction field represents outer sphere degrees of freedom, and the mutual orientation of the nucleobases is explicitely taken into account via the Slater-Koster rules. Furthermore, we aim at the computation of the energetics of the charge-transfer reaction in the absence of an electric field, whereas Conwell and Rakhmanova have focused on the drift mobility within a dynamic picture.

3. Results and Discussion

We have computed the parameters relevant to hole transfer in DNA using the modified SSH model described in the previous section for the following systems, all containing 16 base pairs. For all model systems, we consider both the A and the B form of the DNA. First, we have a single G and a G triplet embedded in a sequence of A−U base pairs. The G and the GGG structures are separated by n A−U pairs, where $0 \le n \le 4$ for the A and $0 \le n \le 7$ for the B form. Second, for $2 \le n \le 4$, every other

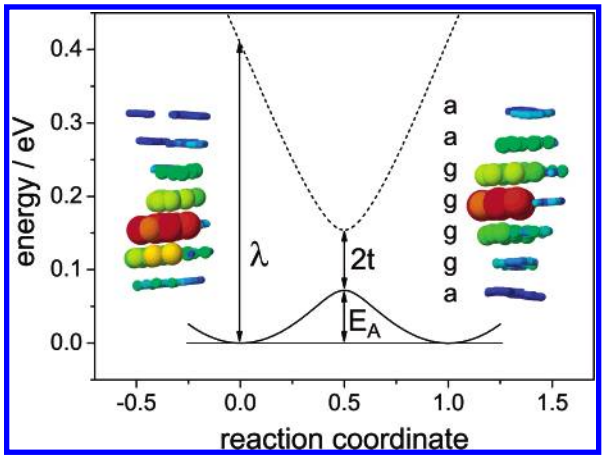

Figure 3. Energy profile for hole transfer between two neighboring guanines. Bottom, ground state; top, first excited state. Inserts, charge distribution for the polaron states at the minima; the sizes of the spheres are proportional to the logarithm of the excess charge.

TABLE 1: DNA Sequences Used for the Computation of Superexchange Charge Transfer Parameters

model	sequence
G0	AAAAAAGGGGAAAAAA
G1	AAAAAGAGGGAAAAAA
G2	AAAAAGAAGGGAAAAA
G3	AAAAGAAAGGGAAAAA
G4	AAAAGAAAAGGGAAAA
G5	AAAAGAAAAAGGGAAA
G6	AAAGAAAAAAGGGAAA
G7	AAAGAAAAAAAGGGAA
G1′	AAAAAGUGGGAAAAAA
G2′	AAAAAGAUGGGAAAAA
G3′	AAAAGAUAGGGAAAAA
G4′	AAAAGAUAUGGGAAAA
A16	AAAAAAAAAAAAAAAA
G16	GGGGGGGGGGGGGGGG
AU8	AUAUAUAUAUAUAUAU
CG8	CGCGCGCGCGCGCGCG

A−U pair is replaced by U−A. These systems are similar to the DNA oligomers investigated experimentally by Giese and co-workers and we refer to them as G0-G7 and G1′−G4′. Finally, we focus on regular, repeating sequences such as A_{16}, G_{16}, $(AU)_8$, and $(GC)_8$. The sequences described here are also listed in Table 1.

In the SCF computations, we proceed as follows. Each base is considered to be a potential center of charge localization. Hence, we use initial conditions that reflect the bond order (or bond length) distribution of a single charged base a and that of the neutral bases for the remaining 31 centers; here the index a may be varied. Whenever the initial charge is localized on a guanine base of the G0-G4 sequences, the SCF procedure rapidly converges into the final charge distribution. In Figure 3, we display the charge distributions of two distinct SCF minima of the G0 oligomer in its B form. The emerging excess hole charge is strongly localized and is essentially confined to a single guanine. The adjacent bases each carry a net excess hole charge, as compared to the neutral molecule, of the order of one percent of that of center of localization. We note, however, that this localization behavior of the hole does not imply a similar strong localization of other valence band orbitals, which may support electronic coupling. If we apply initial conditions appropriate to an A, C, or U cation, the SCF convergence is slower than that observed for the G cation, and the charge finally localizes on the nearest G residue. Thus, in the systems studied here, the guanine bases operate as charge traps and form the centers of a polaron state. As a consequence,

intermediate A−U pairs act as barriers for tunneling. We note that no significant delocalization within clusters of G bases has been observed.

We will now quantify these findings by accessing a cross section of the potential energy surface relevant to hole transfer between two G bases by a linear synchronous transit (LST) approach.[41] In doing so, we adopt a procedure that contains elements of the aforementioned adiabatic charging process and the application of an interpolation method to charge transfer, which we have recently tested for a multicenter hopping problem.[28] The bond orders that characterize each of the minima, which we may denote as X and Y, are given by $\{\bar{n}_{1,1,X}; \bar{n}_{1,2,X}; ...; \bar{n}_{N-1,N,X}; \bar{n}_{N,N,X}\}$ and $\{\bar{n}_{1,1,Y}, \bar{n}_{1,2,Y}, ..., \bar{n}_{N-1,N,Y}, \bar{n}_{N,N,Y}\}$, respectively. The interpolation is performed by setting the bond order of the Hamiltonian 2.2 as $\bar{n}_{i,j} = \Gamma\bar{n}_{i,j,X} + (1 - \Gamma)\,\bar{n}_{i,j,Y}$; where the interpolation parameter Γ serves as a reaction coordinate. The charge orders are interpolated in the same way. The resulting energy profiles for hole transfer from a single G to the first guanine of a GGG cluster are displayed in Figure 3 for the B form of the G0 model.

The potential energy curves displayed in Figure 3 have the familiar shape of two parabola which experience a level repulsion. From these, the parameters relevant to Marcus' theory of charge transfer in a two-site donor−acceptor system can be immediately extracted. For G0, we obtain a reorganization energy $\lambda = 411.2$ meV, an activation barrier $E_a = 71.7$ meV and an electronic tunnel splitting $t = 41.2$ meV. From a similar analysis, it follows that an intermediate A−U pair (G1 model) does not strongly affect the reorganization energy ($\lambda = 397.3$ meV), whereas the activation barrier slightly increases to 104.7 meV, and the electronic tunnel matrix element is strongly reduced to 5.6 meV. We observe an additional reduction down to 0.11 meV for the G2 model with two intervening A−U base pairs. Whenever excited states experience an avoided level crossing which leads to slightly different values for the donor and the acceptor reorganization energies, we report averages of these two values. The reorganization energies are determined by the strength of the Hubbard parameters that characterize the inner and outer sphere interaction terms, U_{ee} and U_{SSH}. We use $U_{SSH} = 0.32$, as in the original SSH model, and treat U_{ee} as an adjustable parameter of about 1 eV.[25] The experimental reorganization energies for photoexcited charge-transfer lie in the range of 0.38 to 0.48 eV[42] and can be reproduced by $U_{ee} = 0.8$ eV. Even in the total absence of outer sphere contributions, the activation barriers are only lowered by a factor of 2, and the hopping rates increase by 1 to 2 orders of magnitude.

For all models resembling those used by Giese and co-workers, the minimum spatial separartion of the donor and the acceptor base, the corresponding average separation (where only nonhydrogen atoms have been considered), E_a and t are listed in the Tables 2 and 3. From these parameters, the hopping rates can be estimated via[11]

$$k_{CT} = \frac{t^2}{\hbar}\sqrt{\frac{2\pi}{\lambda k_B T}}\exp\left(-\frac{E_a}{k_B T}\right) \qquad (3.1)$$

The thus computed numerical values are also listed in Tables 2 and 3. For nearest-neighbor hopping between guanines, a rate of 6.2×10^{14} s^{-1} emerges. For this very fast rate, nonadiabaticity corrections may become necessary,[43] so that our computed rate for the G0 sequence has to be considered as an upper boundary provided the system does not undergo thermal or dynamical delocalization. As a general trend, the hopping rates decrease by 1−2 orders of magnitude with each additional A−U or U−A pairs separating the guanines. With three or four of these intervening pairs, k_{CT} becomes as small as 10^5 s^{-1}. Comparing to experiments, the G2 model rate of 2.4×10^8 s^{-1} is close to the estimate of Bixon et al.[7] (10^9 s^{-1}), which follows from an analysis of Giese's results. Photochemical experiments, on the other hand, suggest 10^7 s^{-1} for hole recombination in the G1 sequence[44] in obvious disagreement with the results of Bixon and co-workers[7] and the computations reported here.

TABLE 2: DNA A Form Charge Transfer Parameters for Systems Containing Four G−C Base Pairs[a]

model	r_{min} (Å)	$\bar{r}$ (Å)	E_a (meV)	t (meV)	k_{CT} (s^{-1})
G0	3.06	4.90	55.0	57.6	6.2×10^{14}
G1	6.04	8.38	92.7	11.9	5.0×10^{12}
G2	8.88	11.73	95.8	1.8	1.2×10^{11}
G3	11.53	14.64	97.2	0.30	3.2×10^{9}
G1′	6.04	8.38	98.6	5.4	9.7×10^{11}
G2′	8.88	11.73	99.0	0.90	2.6×10^{10}
G3′	11.53	14.64	97.9	0.078	2.1×10^{8}

[a] Minimum interbase separation r_{min}, average interbase separation $\bar{r}$, activation barrier E_a, electronic tunnel matrix element t and room temperature ($T = 293$ K) charge transfer reaction coefficient k_{CT}.

TABLE 3: DNA B Form Charge Transfer Parameters for Systems Containing Four G−C Base Pairs[a]

model	r_{min} (Å)	$\bar{r}$ (Å)	E_a (meV)	t (meV)	k_{CT} (s^{-1})
G0	3.24	4.61	71.7	41.2	5.2×10^{14}
G1	6.56	7.85	104.7	5.6	7.9×10^{11}
G2	9.84	11.24	110.1	0.11	2.4×10^{8}
G3	13.47	14.60	110.3	4.8×10^{-3}	4.6×10^{6}
G4	16.96	17.92	110.3	1.0×10^{-3}	2.0×10^{5}
G1′	6.56	7.85	109.6	1.9	7.5×10^{10}
G2′	9.84	11.24	110.1	0.12	2.9×10^{8}
G3′	13.47	14.60	111.5	3.7×10^{-3}	2.6×10^{6}
G4′	16.96	17.92	110.2	1.7×10^{-3}	5.8×10^{5}

[a] Minimum interbase separation r_{min}, average interbase separation $\bar{r}$, activation barrier E_a, electronic tunnel matrix element t and room temperature ($T = 293$ K) charge transfer reaction coefficient k_{CT}.

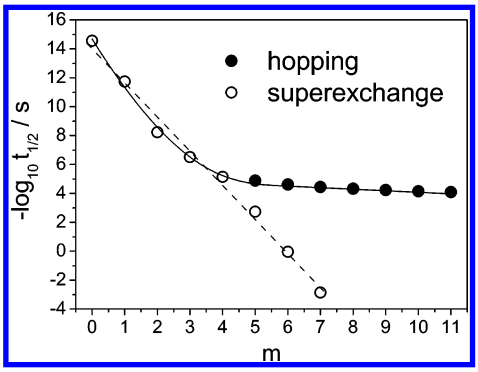

Figure 4. Characteristic time scales for superexchange (empty circle) and hopping (full circle) transport processes between two guanines as a function of the number of intervening adenines, m. The solid line is a guide to the eye, the dashed line represents a least-squares fit to the Marcus−Levich−Jortner relation, eq 3.2.

For the B form, the decadic logarithm of the inverse half-life, which differs from k_{CT} by a factor of ln 2, as a function of intervening A−U pairs is presented in Figure 4. From a linear least-squares fit, we obtain the decay parameter of the Marcus-Levich-Jortner relation

$$k_{CT} \propto \exp(-\beta R) \qquad (3.2)$$

as $\beta = 1.38 \pm 0.13$ Å^{-1}, which is close to the upper boundary of the interval 0.1 Å$^{-1} < \beta < 1.4$ Å reported for experiments.[45] For the A form, a similar picture emerges. Within the numerical

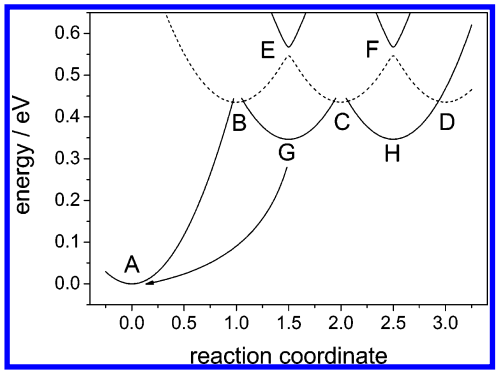

Figure 5. Potential energy surfaces for processes involving adenine-adenine hopping. The arrow indicates the decay channel B → G. For details, see Table 4 and text.

accuracy obtainable to locate the transition state, the coupling between two guanines separated by seven or more A−U pairs vanishes. From a qualitative perspective, charge transfer in the A form within the sequences GA_nGGG is generally faster than in the B form for $n < 4$. The driving force ΔG for hole transfer from a single G to a GGG triplet as computed in our model is small, it typically amounts to less than 10 meV. Consequently, there is only a small preference corresponding to the Boltzmann weight of a triplet G compared to an isolated G with $w_3/w_1 \simeq 0.82$ at room temperature (considering the degeneracy factor). Larger stabilization energies of a GGG wrt to a single G have been reported in the literature, they range from 80 meV (photochemical experiments[46]) over 130 meV (semiempirical calulations[15]) to 680 meV (ab initio values[16]). The reaction enthalpy becomes important once the computation of oxidation yields, e.g., in G doublets or triplets, is intended,[47] and it can also be incorporated in the model suggested here via a shift of the diagonal nucleobase parameters. It does, however, not play a dominant role for the computation of transfer rates and their dependence on the interbase distance and has been neglected here.

Can the extended SSH Hamiltonian, eqs 2.2 and 2.4, also account for long-range transport via a different mechanism? To address this question, we consider the oligomer A_3GA_{12}. Again, an excess positive charge can predominantly localize on the guanine nucleobase. Depending on the initial conditions and on the precise value of the difference between the adenine and the guanine oxidation potential (here set to 0.44 eV), holes can also localize on adenines separated from the guanine base by at least two A−U Watson−Crick pairs. The resulting charge-transfer potential energy surface can be scanned using the LST approach referenced above. It is shown in Figure 5 for transport involving the bases $G^{(4)}$, $A^{(7)}$, $A^{(8)}$, and $A^{(9)}$, where the superscript indicates the position of the base within the sequence of the oligomer. Integer values of the reaction coordinate $R = 0$, 1, 2, and 3 refer to charge localization on these nucleobases, respectively. For $R = 0$, the hole is centered on the guanine base, the corresponding minimum is labeled as A. It can be transferred to $A^{(7)}$ ($R = 1$, B minimum) requiring a reaction energy of $\Delta E = \Delta E° = 436$ meV. This process, as the corresponding backward reaction, is almost activationless. We compute an effective tunnel splitting of 2.6 meV and reaction coefficients of $k_{AB} = 5.4 \times 10^4\ s^{-1}$ and $k_{BA} = 2.0 \times 10^{12}\ s^{-1}$ using eq 3.1. Once a hole is temporarily trapped in the B minimum, the backward reaction to A competes with forward hopping to the next adenine ($A^{(8)}$, minimum C, $R = 2$) along the potential energy surface displayed as a dotted line. This hopping process is characterized by a vanishing driving force and a activation barrier of $\Delta E = E_a = 111$ meV (saddle point E). With a comparatively large tunnel splitting of 20.8 meV, we arrive at a hopping rate of $k_{BC} = 1.5 \times 10^{12}\ s^{-1}$, which is close to k_{BA}. Consecutive hops such as that from minimum C to D ($R = 3$, $A^{(9)}$) via the saddle point F exhibit the same energy parameters and reaction coefficients.

TABLE 4: Charge Transfer Parameters for Elementary Reaction Steps Involving Adenine Hopping Transport[a]

reaction	t (meV)	E_a (meV)	k_{CT} (s^{-1})
A → B	1.3	436	5.4×10^4
B → A	1.3	zero	2.0×10^{12}
B ⇌ C	10.4	111	1.5×10^{12}
B → G	0.74	zero	6.6×10^{11}
C ⇌ D	10.4	111	1.5×10^{12}
C → G	4.1×10^{-2}	zero	2.0×10^9
C → H	3.9×10^{-2}	zero	1.8×10^9
D → H	3.8×10^{-3}	zero	1.7×10^7

[a] Reaction step (cf. Figure 5), activation energy E_a, effective electronic tunnel matrix element t and room temperature ($T = 293$ K) charge transfer reaction coefficient k_{CT}.

As an additional decay channel that exits the potential energy surface for adenine−adenine hopping, we find processes in which the hole delocalizes over two adenines (minima G and H at $R = 1.5$ and $R = 2.5$, respectively). We have used the density matrix at either of these minima as a starting point of the SCF procedure, which ultimately converges into a charge and bond order distribution that is identical to the minimum A, i.e., charge localization on guanine. In addition, a three-dimensional interpolation involving the state $G^{(4)}$ and the adenines $A^{(7)}$ and $A^{(8)}$ shows that backward transfer from the minimum G to the guanine base A is activationless. Consequently, this and related processes compete with adenine−adenine hopping transport. The potential energy surface participating in this backward reaction is, however, only weakly coupled to those representing adenine-adenine hopping. For the corresponding step B → G, we obtain a reaction coefficient of $6.6 \times 10^{11}\ s^{-1}$. In contrast to adenine−adenine hopping, the exit path rate decreases with increasing adenine-guanine distance down to $\sim 2 \times 10^9\ s^{-1}$ for the C → G and the C → H processes, and even further to $1.7 \times 10^7\ s^{-1}$ for the step D → H. Thus, these rates are small compared to adenine-adenine hopping with the exception of the first exit channel, B → G → A. All parameters relevant to the charge-transfer processes discussed here are also listed in Table 4.

The rates computed above are used to analyze charge transfer from one guanine (A) to another (A') via a sequence of intervening A−U base pairs. We use the sequence $A_2GA_MGA_2$ and study the reaction scheme

$$A \rightleftharpoons B \rightleftharpoons C \rightleftharpoons \ldots \rightleftharpoons C' \rightleftharpoons B' \rightleftharpoons A' \qquad (3.3)$$

including the exit channels $B \rightarrow G \rightarrow A$ and $B' \rightarrow G' \rightarrow A'$. Irreversible processes such as trapping have not been taken into account here. The linear system of first-order kinetic differential equations describing the scheme 3.3 can be solved numerically. For an initial oxidation of the left guanine base, we obtain as a result the characteristic time $t_{1/2}$ at which half of the excess charge can be detected at different nucleobases. In Figure 4, we display this quantity as a function of the number of intervening A−U base pairs and compare it to the computed superexchange half-life, k_{CT} ln 2. The crossover between the superexchange and the hopping regime can be found at a time equal to the inverse reaction coefficient of the rate-limiting step of the adenine-adenine hopping mechanism, namely the population of the first adenine, at $\sim 2 \times 10^{-4}$ s. As adenine−adenine hopping can be described by a Poisson process, the

TABLE 5: Electron Transfer Parameters for Regular DNA Sequences[a]

model	form	r_{min} (Å)	$\bar{r}$ (Å)	E_a (meV)	t (meV)	k_{CT} (s^{-1})
A16	B	3.30	4.51	111.1	10.4	2.0×10^{12}
G16	B	3.24	4.61	71.5	41.0	1.7×10^{14}
CG8	B	3.58	6.29	80.1	32.9	7.8×10^{13}
AU8	B	3.46	5.42	59.4	72.2	8.0×10^{14}
A16	A	3.05	4.24	77.7	42.7	1.3×10^{14}
G16	A	3.06	4.90	53.5	56.9	6.9×10^{14}
CG8	A	3.62	7.24	83.2	23.0	3.2×10^{13}
AU8	A	3.35	5.35	61.2	70.6	7.0×10^{14}

[a] Minimum interbase separation r_{min}, average interbase separation $\bar{r}$, activation barrier E_a, electronic tunnel matrix element t and room temperature ($T = 293$ K) charge transfer reaction coefficient k_{CT}.

total hopping rate depends on the number of these pairs via a power law. In contrast, the superexchange rate decreases exponentially with the number of adenines involved, and it becomes slower than the adenine−adenine hopping process if more than four A−U pairs separate two guanines ($k_{CT} < 10^3$ s^{-1}). This estimate of the breakeven point of the two mechanisms involves one more intervening adenine than that of Giese and co-workers.[9] We note that from our calculation, a minimum of five A−U pairs is required not only to induce localization on one of the bridging adenines but also to make hopping from one adenine to the other a process that is roughly as fast as the decay rate of holes thermally excited to the adenine−adenine hopping energy surface. We note that to describe the process of hopping via intermediate adenines, U_{ee} has to be at least as large as assumed here, otherwise the intermediate adenine minima cease to exist. With this constraint and the likely upper limit of U_{ee} given above, we have 0.8 eV $\leq U_{ee} \leq$ 1.2 eV for a physically reasonable description of charge transfer in DNA.[48]

We finally turn to charge transfer in regular systems. These models, A16, G16, AU8, and CG8, are defined in Table 1 and have been studied in their A and B forms. The computed parameters relevant to hole transfer are listed in Table 5. Due to the small activation barrier and the large coupling element resulting from the direct proximity of the bases, they exhibit a large hopping rate both in the A and the B form. Hopping from a C−G to a G−C pair, as compared to G−C to G−C hopping, reduces the charge-transfer rate slightly. Interestingly, in the absence of guanine, i.e., for the A16 and AU8 models, adenine serves as a charge trap for a polaron state, and 16 local minima corresponding to hole localization on this base exist on the potential energy surface. Here, the hopping rates calculated for the alternating sequence, AU8, are larger than those for the more regular model, A16. This statement holds both for the A and the B form.

4. Conclusions

In this work, we have addressed the problem of DNA hole transfer in the electronic ground state from a theoretical and computational perspective. We have extended a standard model for charge transport in doped π electron systems, the SSH Hamiltonian, to account for the presence of heteroatoms, polarization effects, and interbase coupling. The model has been parametrized using ab initio quantum chemical calculations and experimental data. We consider the nonretarded limit, in which inner and outer sphere contributions to charge transfer can be treated on the same footing and an efficient numerical solution of the mean-field approximation to the electronic Hamiltonian is feasible.

In the presence of G−C Watson−Crick pairs, an excess hole charge predominantly localizes on a guanine nucleobase, whereas A, C, and U cannot act as charge traps. The bond lengths within the center of localization are deformed, and a charge reorganization in response to the reaction field part of the Hamiltonian can be computed. Thus, the resulting quasiparticle can be considered as a small polaron, as reasoned by Henderson et al.[49] following a kinetic analysis of their DNA oxidation experiments. A cross-section of the potential energy surface relevant to hole transfer has been computed using a linear synchronous transit approach. It can be analyzed using Marcus' theory of electron transfer; in this manner, the atomistic model presented here can be mapped onto a much simpler two-site system, which in turn allows the approximate calculation of the energy parameters and the reaction coefficient. Computed reorganization energies amount to ∼400 meV, and the maximum activation barrier for charge hopping is ∼100 meV. We reiterate that the only free parameter of our model, U_{ee}, is adjusted to meet the experimental reorganization energy and that the qualitative description of the guanine-guanine hopping process does not depend on its exact numerical value. Inner and outer sphere effects contribute to the reorganization energy in a roughly equal weight. In nonregular DNA strands, effective coupling matrix elements are as large as 50 meV, and they rapidly fall off with an increasing number of adenine bases located between two guanines. The corresponding hopping rates fall off exponentially with increasing interbase distance both for the DNA A and B form. For the B form, a Marcus-Levich-Jortner parameter of 1.38 ± 0.13 $Å^{-1}$ emerges, which lies on the upper side of experimental and theoretical literature values.[45] The results of our model are thus compatible with a short-range guanine−guanine hopping model, where intervening bases give rise to a superexchange mechanism. As we are able to directly compute the electronic tunnel splitting by a nonperturbational, i.e., variational procedure, there is, however, no necessity to explicitely introduce superexchange parameters. The same model provides a potential energy surface relevant to adenine−adenine hopping that can be thermally populated and which determines the conductivity for a larger number of A−U pairs. From this surface, direct hopping to a neighboring guanine or the formation of extended adenine hole states constitute the exit pathes.

The atomistic nature and the chemical specifity of the extended SSH model permit the treatment of a variety of nucleobase arrangements, regardless of their mutual orientation. In contrast to simple phenomenological polaron models with a single site representing a base, an atomistic model has a high predictive power and can be used to analyze models of stacking-fault disorder, quasistatic disorder due to the slow dynamics of the DNA, or hole transfer in DNA−RNA hybrides without any reparametrization.

Acknowledgment. It is a pleasure to thank A. Blumen, T. Friedrich, N. Utz, M. Rateitzak, G. Ganzenmüller, L. Engel, and C.A. Zell for fruitful discussions and helpful comments. We gratefully acknowledge the use of the TINKER[17] and MOLEKEL[37] program packages. Financial support by the Deutsche Forschungsgemeinschaft is gratefully acknowledged.

References and Notes

(1) Treadway, C. R.; Hill, M. G.; Barton, J. K. *Chem. Phys.* **2002**, *281*, 409. Delaney, S.; Barton, J. K. *J. Org. Chem.* **2003**, *68*, 6475.

(2) Fink, H.-W. *Cell. Mol. Life. Sci.* **2001**, *58*, 1.

(3) Arkin, M. R.; Stemp, E. D. A.; Holmlin, R. E.; Barton, J. K.; Hoermann, A.; Olson, E. J. C.; Barbara, P. F. *Science* **1996**, *273*, 475. Hall, D. B.; Holmlin, R. E.; Barton, J. K. *Nature* **1996**, *382*, 731.

(4) Fiebig, T.; Wan, C.; Kelley, S. O.; Barton, J. K.; Zewail, A. H. *Proc. Natl. Acad. Sci. U.S.A.* **1999**, *96*, 1187; *Proc. Natl. Acad. Sci. U.S.A.*

1999, *96*, 6014. Wan, C.; Fiebig, T.; Schiemann, O.; Barton, J. K.; Zewail, A. H. *Proc. Natl. Acad. Sci. U.S.A.* **2000**, *97*, 14052.

(5) Meggers, E.; Kusch, D.; Spichty, M.; Wille, U.; Giese, B. *Angew. Chem., Int. Ed. Engl.* **1998**, *37*, 459. Meggers, E.; Michel-Beyerle, M. E.; Giese, B. *J. Am. Chem. Soc.* **1998**, *120*, 12950.

(6) Fink, H. W.; Schönenberger, C. *Nature* **1999**, *398*, 407. Porath, D.; Bezryadin, A.; de Vries, S.; Dekker, C. *Nature* **2000**, *403*, 635.

(7) Bixon, M.; Giese, B.; Wessely, S.; Langenbacher, T.; Michel-Beyerle, M. E.; Jortner, J. *Proc. Natl. Acad. Sci.* **1999**, *96*, 11713.

(8) Renger, T.; Marcus, R. A. *J. Phys. Chem. A* **2003**, *107*, 8404.

(9) Giese, B.; Amaudrut, J.; Kohler, A. K.; Spormann, M.; Wessely, S. *Nature* **2001**, *412*, 318. Giese, B.; Spichty, M. *ChemPhysChem* **2000**, *1*, 195.

(10) Petrov, E. G.; Shevchenko, Ye. V.; May, V. *Chem. Phys.* **2003**, *288*, 269.

(11) Marcus, R. A. *J. Chem. Phys.* **1956**, *24*, 966; *J. Chem. Phys.* **1956**, *24*, 979; *Annu. Rev. Phys. Chem.* **1964**, *15*, 155.

(12) Voityuk, A. A.; Rösch, N.; Bixon, M.; Jortner, J. *J. Phys. Chem. B* **2000**, *104*, 9740.

(13) Troisi, A.; Orlandi, G. *Chem. Phys. Lett.* **2001**, *344*, 509.

(14) Voityuk, A. A.; Siriwong, K.; Rösch, N. *Angew. Chem.* **2004**, *116*, 634.

(15) Voityuk, A. A.; Jortner, J.; Bixon, M.; Rösch, N. *Chem. Phys. Lett.* **2000**, *324*, 430.

(16) Sugiyama, H.; Saito, I. *J. Am. Chem. Soc.* **1996**, *118*, 7063.

(17) Pappu, R. V.; Hart, R. K.; Ponder, J. W. *J. Phys. Chem. B* **1998**, *102*, 9725. Dudek, M. J.; Ramnarayan, K.; Ponder, J. W. *J. Comput. Chem.* **1998**, *19*, 548. Kong, Y.; Ponder, J. W. *J. Chem. Phys.* **1997**, *107*, 481. Ponder, J. W.; Richards, F. M. *J. Comput. Chem.* **1987**, *8*, 1016.

(18) Voityuk, A. A.; Siriwong, K.; Rösch, N. *Phys. Chem. Chem. Phys.* **2001**, *3*, 5421.

(19) Su, W. P.; Schrieffer, J. R.; Heeger, A. J. *Phys. Rev. Lett.* **1979**, *42*, 1698; *Phys. Rev. B* **1980**, *22*, 2099.

(20) Torii, H. J. *Phys. Chem.* **2000**, *104*, 413. Zao, H.; An, Z.; Wu, C. Q. *Synth. Met.* **2003**, *135*, 535.

(21) Ma, J.; Yuan, R.-K. *Phys. Rev. B* **1988**, *57*, 9343. Huang, Y.; Okada, M.; Tanaka, K.; Yamabe, T. *Sol. State Comm.* **1996**, *97*, 303. Jiang, J.; Dong, J.; Wan, X.; King, D. Y. *Phys. Lett. A* **1998**, *241*, 274.

(22) Rateitzak, M.; Koslowski, T. *Chem. Phys. Lett.* **2003**, *377*, 455.

(23) Ness, H.; Shevlin, S. A.; Fisher, A. J. *Phys. Rev. B* **2001**, *63*, 125422.

(24) Micnas, R.; Ranninger, J.; Robaskiewicz, S. *Rev. Mod. Phys.* **1990**, *62*, 113. Shen, S.-Q. *Int. J. Mod. Phys. B* **1998**, *12*, 709. Mancini, F.; et al. *Int. J. Mod. Phys. B* **1996**, 1717.

(25) Utz, N.; Koslowski, T. *Chem. Phys.* **2002**, *282*, 389.

(26) Koslowski, T. *J. Chem. Phys.* **2000**, *113*, 10703; *Z. Phys. Chem. NF* **2001**, *215*, 1625 27. Koslowski, T. *Phys. Chem. Chem. Phys.* **2003**, 5, 2197.

(27) Koslowski, T.; Jurjiu, A.; Blumen, A. J. *Phys. Chem. B* **2004**, *108*, 3283.

(28) Goodenough, J. B.; in Brown, D. B. *Mixed valence compounds*; D. Reidel: Dordrecht, The Netherlands, 1980.

(29) Georges, A.; Kotliar, G.; Krauth, W.; Rozenberg, M. J. *Rev. Mod. Phys.* **1996**, *68*, 13.

(30) See, for example: May, V.; Kühn, O. *Charge and energy transfer dynamics in molecular systems*; Wiley-VCH: Berlin, 2000.

(31) Kuharski, R. A.; Bader, J. S.; Chandler, D.; Sprik, M.; Klein, M. L.; Impey, R. W. *J. Chem. Phys.* **1988**, *89*, 3248. Bader, J. S.; Chandler, D. *Chem. Phys. Lett.* **1989**, *157*, 501. Bader, J. S.; Kuharski, R. A.; Chandler, D. *J. Chem. Phys.* **1990**, *93*, 230.

(32) Hwang, J.-K.; Warshel, A. *J. Am. Chem. Soc.* **1987**, *109*, 715.

(33) Streitwieser, A. *Molecular Orbital Theory for Organic Chemists*; Wiley and Sons: New York, 1961.

(34) Frisch, M. J.; Trucks, G. W.; Schlegel, H. B.; Scuseria, G. E.; Robb, M. A.; Cheeseman, J. R.; Montgomery, J. A., Jr.; Vreven, T.; Kudin, K. N.; Burant, J. C.; Millam, J. M.; Iyengar, S. S.; Tomasi, J.; Barone, V.; Mennucci, B.; Cossi, M.; Scalmani, G.; Rega, N.; Petersson, G. A.; Nakatsuji, H.; Hada, M.; Ehara, M.; Toyota, K.; Fukuda, R.; Hasegawa, J.; Ishida, M.; Nakajima, T.; Honda, Y.; Kitao, O.; Nakai, H.; Klene, M.; Li, X.; Knox, J. E.; Hratchian, H. P.; Cross, J. B.; Adamo, C.; Jaramillo, J.; Gomperts, R.; Stratmann, R. E.; Yazyev, O.; Austin, A. J.; Cammi, R.; Pomelli, C.; Ochterski, J. W.; Ayala, P. Y.; Morokuma, K.; Voth, G. A.; Salvador, P.; Dannenberg, J. J.; Zakrzewski, V. G.; Dapprich, S.; Daniels, A. D.; Strain, M. C.; Farkas, O.; Malick, D. K.; Rabuck, A. D.; Raghavachari, K.; Foresman, J. B.; Ortiz, J. V.; Cui, Q.; Baboul, A. G.; Clifford, S.; Cioslowski, J.; Stefanov, B. B.; Liu, G.; Liashenko, A.; Piskorz, P.; Komaromi, I.; Martin, R. L.; Fox, D. J.; Keith, T.; Al-Laham, M. A.; Peng, C. Y.; Nanayakkara, A.; Challacombe, M.; Gill, P. M. W.; Johnson, B.; Chen, W.; Wong, M. W.; Gonzalez, C.; Pople, J. A. *Gaussian 03*, revision B.04; Gaussian, Inc.: Pittsburgh, PA, 2003.

(35) Seidel, C. A. M.; Schulz, A.; Sauer, M. H. M. *J. Phys. Chem.* **1996**, *100*, 5541. Steenken, S.; Jovanovic, S. V. *J. Am. Chem. Soc.* **1997**, *119*, 617.

(36) Portmann, S.; Lüthi, H. P. *CHIMIA* **2000**, *54*, 766.

(37) Chadi, D. J.; Cohen, M. L. Phys. Stat. Sol. B **1975**, *68*, 405. Harrison, W. A. *Electronic structure and the properties of solids*; Freeman: San Francisco, CA, 1980.

(38) Slater, J. C.; Koster, G. F. *Phys. Rev.* **1954**, *94*, 1498.

(39) Conwell, E. M.; Rakhmanova, S. V. *Proc. Natl. Acad. Sci. U.S.A.* **2000**, 97, 4556. Rakhmanova, S. V.; Conwell, E. M. *J. Phys. Chem. B* **2001**, *105*, 2056.

(40) Rauhut, G.; Clark, T. *J. Am. Chem. Soc.* **1993**, *115*, 9127. Gröppel, M.; Roth, W.; Clark, T. *Adv. Mater.* **1995**, *7*, 927.

(41) Harriman, A. *Angew. Chem., Int. Ed. Engl.* **1999**, *38*, 945.

(42) Zusman, L. D. *Chem. Phys.* **1980**, *49*, 295.

(43) Lewis, F. D.; Liu, X.; Miller, S. E.; Hayes, R. T.; Wasielewski, M. R. *Nature* **2000**, *406*, 51.

(44) Giese, B. *Acc. Chem. Res.* **2000**, *33*, 631 and references therein.

(45) Lewis, F. D.; Xiaoyang, T. W.; Letsinger, R. L.; Grennfield, S. R.; Miller, S. E.; Wasielewski, M. R. *J. Am. Chem. Soc.* **2000**, *122*, 2889.

(46) Berlin, Y. A.; Burin, A. L.; Ratner, M. A. *J. Am. Chem. Soc.* **2001**, *123*, 260.

(47) In that interval, the reorganization energy shows a linear dependence on the reaction field strength. For the G1 model, we find $\lambda = 447$, 484, 523, 565, and 610 meV for $U_{ee} = 0.8$, 0.9, 1.0, 1.1 and 1.2 eV, respectively.

(48) Henderson, P. T.; Jones, D.; Hampikian, G.; Kan, Y.; Schuster, G. B. *Proc. Natl. Acad. Sci.* **1999**, *96*, 8353.